Long-term prediction for vertical bending moment utilizing the AIS data and global wave data

Masayoshi Oka[1] · Chong Ma[1]

Abstract

Utilizing the AIS data and global ocean wave data, the vertical bending moment (*VBM*) that acted on the actual ships was clarified. The long-term prediction was performed based on the short-term analysis of *VBM* on actual ships in the worldwide sea area. The effect of storm avoidance operations on wave height is about 22% in worldwide sea area. The effect on *VBM* in the worldwide sea is about 16%. These effects are greater than that in North Atlantic.

List of Symbols

AIS	Automatic identification system
BC	Bulk carriers
CS	Container ships
DLA	Direct load analysis
DWT	Deadweight tonnage
F_A	Component of F_{OP} and/or F_H related to the sea area
F_H	Operational coefficient on wave height
F_{OP}	Operational coefficient on wave load
F_R	Component of F_{OP} related to the storm avoidance operations on wave load
F_{RH}	Component of F_R due to wave height
F_{RO}	Component of F_R due to other than wave height
f_R	Factor on wave load related to operation regulated by the design rule by IACS
GWS	Global wave statistics
GPV	Grid point value
H	Significant wave height
IACS	International Association of Classification Societies
JMA	Japan meteorological agency
L	Length of the ship
NA	North Atlantic
OT	Oil tankers
$p(R)$	Probability density function for the R during long-term
P	Exceedance probability for the significant wave height
Q	Long-term exceedance probability for the wave load
q	Short-term exceedance probability for the wave load
R	Standard deviation of wave load in the short-term sea
RAO	Response amplitude operator
S.M.	Safety margin for ocean wave data
T	Average wave period
T_P	Peak wave period
T_Z	Average zero-crossing wave period
V	Ship speed
VBM	Vertical bending moment in wave
WW	Worldwide sea
θ	Wave direction
χ	Relative wave direction

✉ Masayoshi Oka
moka@m.mpat.go.jp

1   National Maritime Research Institute, 6-38-1 Shinkawa, Mitaka, Tokyo 181-0004, Japan

1 Introduction

The wave load acting on the ship is believed to be lower than those estimated in the design phase due to the operation or storm avoidance including the weather routing and safe maneuverings such as speed change or headings in rough seas. These are called "storm avoidance" in this paper. Regarding the evaluation of operational effects, Soares constructed a probabilistic model of storm avoidance operations

based on the results of interviews with ship operators and conducted a Monte Carlo simulation [1]. They found that the impact of storm avoidance operations on wave load is 25% at maximum. Vettor et al. analyzed encounter wave data from ship reports and showed that storm avoidance operations could reduce wave height by about 20% [2].

This effect has not been considered in previous designs for safety design criteria because of the uncertainty of ship operation. However, in recent years there have been some design rules quantitively specifying the operational effect on wave load. The design rules for the container ships have regulated the operational factor $f_R = 0.85$ for the design wave load to evaluate the ultimate strength [3].

Due to the operational effects, the wave load that acts on ships in service is lower than the load assumed in the design, which can be quantitively concerned by the operational factor. It is known that the operational effects occur for most ships in service, even though these effects vary from ship to ship. If the design load is determined based on ships that have encountered many severe storms, more steel for the hull construction becomes necessary, and the ship's weight will increase, leading to lower transportation fuel efficiency. To pursue environmentally friendly and lightweight ships with enough structural safety, it is necessary to determine the operational coefficient based on objective data.

In recent years, the Automatic Identification System (AIS) data for the global ocean obtained from satellites has become accessible more easily [4]. Several studies have been conducted to identify the sea conditions that ships encounter using satellite AIS data. Vitali et al. combined satellite AIS data and global ocean wave data to examine the relationship between the speed loss and wave profile. They proposed a method to predict the speed loss by combining it with a questionnaire for operators [5]. Tu et al. conducted an early-stage study to utilize satellite AIS data for machine learning to support maritime safety, security, and maritime transport efficiency [6]. Miratsu et al. showed the operational effects on wave heights that ships encountered and clarified the probability of ship speed and relative wave direction in waves [7]. Sasmal et al. developed a ship maneuvering model for storm avoidance and predicted the encounter waves [8]. They reconstructed the frequency of wave occurrence for 25 years. Ruth et al. clarified the relationship between fatigue damage of hull and ship maneuvers, such as avoidance of rough weather, ship speed, and headings in rough weather, using AIS data and hindcast wave data [9].

To clarify the significance of the operational effects, a data driving research is conducted utilizing big data, which consists of the position of ships in-service collected from the AIS data [10] and the global ocean wave data at any locational point during a specific period [11, 12]. Compositing AIS data and wave data, the parameters representing short-term sea conditions that ships encountered, and the

vertical bending moment (*VBM*) acted on the container ships [11], the bulk carriers, and the oil tankers [12] in-service were estimated by numerical simulation based on the strip method. We indicated that the f_R is valid based on the data. However, since previous studies have limited the ocean area to the North Atlantic, evaluation of the world-wide area was still a challenge. In addition, probabilistic evaluation, such as long-term prediction, was not possible for wave load. In this research, firstly, the load reduction effect of avoiding stormy weather is studied for global sea areas. Then, the difference in load reduction effect by sea area is investigated. Finally, a method for long-term prediction of wave load on ships in service is proposed, and a probabilistic evaluation is performed.

In this study, the linear strip method was utilized to estimate the wave loads on individual ships. According to the linear strip method, the velocity potential and the load acting on the hull can be solved efficiently by approximating the boundary problem based on the slender body assumption [13–16]. Since the 1970s, when the well-known Salvesen-Tuck-Faltinsen (STF, [17]) was proposed, the strip method has undergone significant development. Kashiwagi [18–20] has published a more enhanced strip method, called the Enhanced Unified Theory (EUT), by taking into account the influence of the second-order drift force and surge mode. A simplified EUT based on the far-field method to calculate the added resistance has been suggested by Amini-Afshar et al. [21]. Xia et al. [22] have proposed a nonlinear time domain strip method to predict the ship's motion and structural response under large waves. All of the above research has provided a comparison between calculation results based on the proposed strip method and experimental test results, and the prediction accuracy of the strip method has been proved. In this paper, as tremendous ship data in the global ocean is examined, the linear strip method was adopted to achieve high computational efficiency [23]. Detailed information about the utilized strip method can be found in the literature [24], where the numerical prediction accuracy is validated using data from a tank test. Although there are still technical challenges for roll motion and following waves in the utilized numerical model, vertical motions (pitch and heave) and *VBM* can be estimated satisfactorily while considering the nonlinear effects of the hull shape [25].

Figure 1 shows the overall flowchart of this research. In this study, the short-term wave conditions that actual ships encountered are obtained based on global ocean wave data and the AIS data in the worldwide sea area. The vertical bending moment (*VBM*) acted on actual ships is estimated utilizing the linear strip method. To perform long-term predictions utilizing the data from multiple ships, *VBM* was normalized using design loads from direct strength calculations.
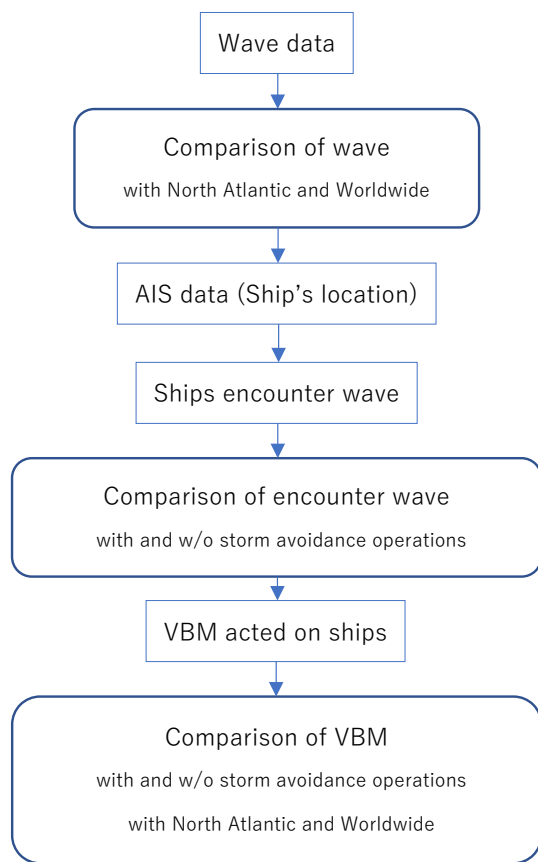
Fig. 1 Overall flowchart of this research

2 Wave data and AIS data

2.1 Wave data

Table 1 shows the summary of the global ocean wave database "Grid Point Value (GPV) of the Japan Meteorological Agency (JMA) [26]". This database is freely accessible. This study uses 2 years of data from 2016 to 2017. The duration of the short-term sea condition is assumed to be 1 h. The value of the short-term parameter is set constant for 6 h because JMA/GPV is 6 h in the interval. The average wave period(T) is expressed in terms of the peak wave period (T_P), so it was converted to the average zero-crossing wave period

Table 1 Summary of global ocean wave database [26]

Area	E0.0°~E359.5°, S75.0°~N75.0°
Mesh (Area/Time)	0.5 degrees (abt. 50 km)/6 h
Element	Significant wave height (H), Peak wave period (T_P), Wave direction (θ)
Data	Nowcast

(T_Z) according to Eq. 1 [27], which gives an approximate relationship between the peak period and the average zero-crossing period.

$$T_Z = 0.71T_P \tag{1}$$

Figure 2 shows the result of the statistical analysis of the global ocean wave data JMA/GPV. P means the long-term exceedance probability of the significant wave height (H). WW denotes worldwide sea area based on the global ocean wave database. NA represents the area 8, 9, 15, 16 of global wave statistics (GWS) [28] according to the guideline of IACS/Rec.34 [29]. The exceedance probabilities of wave height (H) in each sea area were obtained by the frequency distribution of wave height (H) at all locational points included in each sea area. For $P = 10^{-5}$ which corresponds to the maximum recurrence period of 25 years, the ratio of wave height (H) between WW and NN is about 0.92,

For reference, the wave diagram recommended by IACS (IACS/Rec.34 [29]) is shown in Fig. 2 as well. It is found that, the wave height (H) of IACS/Rec.34 is much higher (about 15%) than that of JMA/GPV. This difference can be regarded as a safety margin set to cover the uncertainty of weather data in the design. In this paper, the coefficient of safety margin for ocean wave data ($S.M.$) is determined by Eq. 2.

$$S.M. = 0.15 \tag{2}$$

2.2 AIS data

Table 2 shows the summary of the AIS data. Two years of worldwide sea area data (the commercial satellite AIS data service provided by Spire/Exact earth [30]) with wave information is utilized. The time interval is set to 1 h. As the data
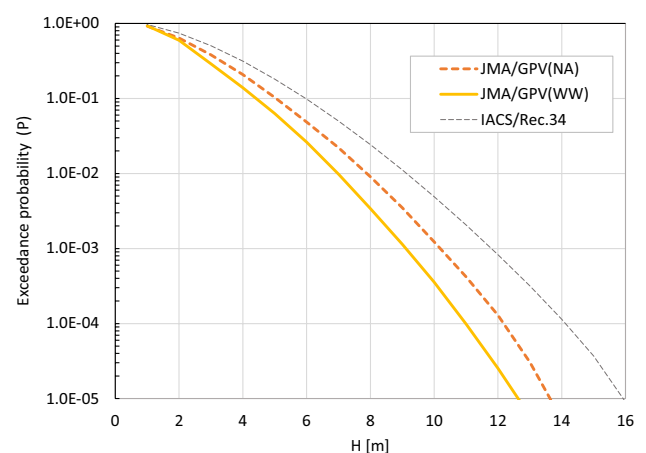

Fig. 2 The exceedance probability of the significant wave height of global ocean wave data

Table 2 Summary of AIS data

Period	2016/1/1/0:00 ∼ 2017/12/31/23:59
Area	Worldwide
Container Ship	4886
Bulk Carrier	9852
Oil Tanker	2697
Total (Analyzed)	17,435
Ship data	IMO number, Name, Kind, Length, Breadth, Draught, DWT, etc
Navigation data	Time, Location (Longitudinal and Latitude), Heading, Speed, etc

on the ship's position is usually obtained in shorter than 1-h time intervals, the average value for 1 h is applied. And in this study, the container ships (CS), the bulk carriers (BC), and the oil tankers (OT), with enough long lengths (longer than 100 m) are investigated. Figures 3 and 4 show the distribution of displacement and length of the sample ships, separately.

3 Definition of operational coefficient

In this study, the long-term maximum expected value of *VBM* for ultimate strength evaluation considering the operational effect is expressed by Eq. 3.

$$VBM = (1 - S.M.) * F_{OP} * VBM_{DLA} \tag{3}$$

F_{OP} means the operational coefficient on wave load. VBM_{DLA} corresponds to the long-term predicted value calculated by the guidelines of the classification society for direct load analysis [31]. According to the guideline, IACS/Rec.34 is applied as the wave diagram, the uniform distribution (all headings) is applied as the relative wave direction, and 5knots (constant) is utilized for the ship speed. The number of waves that the ship will encounter in 25 years is assumed to be 10^8.

F_{OP} is expressed by Eq. 4 by dividing it into a component depending on the difference in the sea area (F_A) and a component depending on the weather routing including the storm avoidance operations (F_R).

$$F_{OP} = F_A * F_R \tag{4}$$

Here, F_A denotes the wave height ratio between the target sea area and the North Atlantic area. It is 1.0 in the NA and 0.92 in WW according to Fig. 2. F_R can be expressed by Eq. 5 by dividing it into a component depending on wave height (F_{RH}) and the influence factor (F_{RO}) of wave period, wave direction, and ship speed.
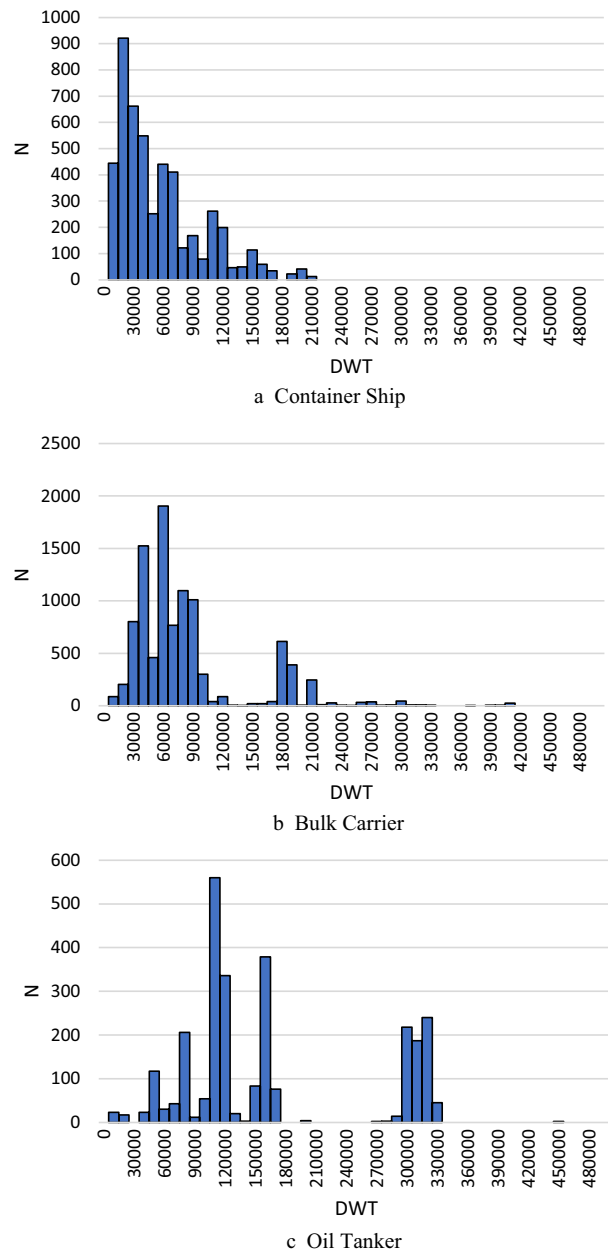

Fig. 3 Distribution of the DWT of sample ships

$$F_R = F_{RH} * F_{RO} \tag{5}$$

The operational coefficient on wave height (F_H) can be also expressed by Eq. 6 in the same form as Eq. 4.
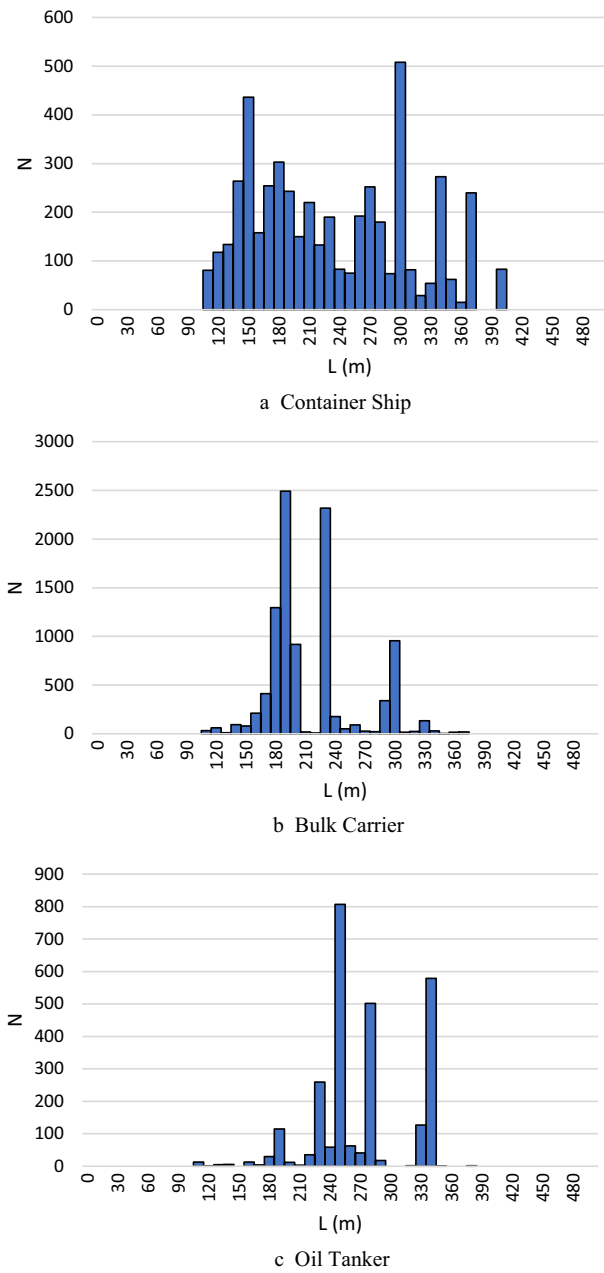
$$F_H = F_A * F_{RH} \tag{6}$$

Fig. 4 Distribution of the length of sample ships

Fig. 5 Exceedance probability of significant wave height that ships encountered

4 Ships encounter wave

Figure 5 shows the probability distribution of the significant wave height that ships encountered. *P* means long-term exceedance probability of the significant wave height. The operational effect on wave height can be confirmed by about 20%, which can be obtained by the rate of encounter wave (ENC) and global ocean wave (JMA).

Figure 6 presents the significant wave height that ships encountered corresponding to $P = 10^{-5}$. A reproduction period of 25 years is assumed to be 10^5. F_{RH} means the

component of F_H related to storm avoidance which can be obtained by Eq. 6. F_{RH} can be also derived by the rate of encounter waves (ENC) and global ocean wave data (JMA) shown in Fig. 6. The operational coefficients are listed in
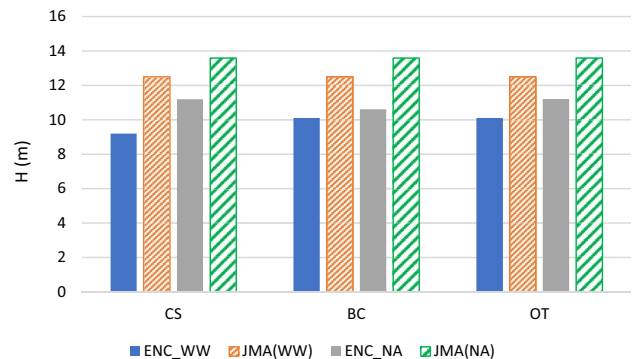
Fig. 6 The significant wave height that ships encountered corresponding to $P = 10^{-5}$

Table 3 Operational coefficients on wave height (F_H) and its component

		F_H	F_A	F_{RH} ($= F_H / F_A$)
CS	WW	0.68	0.92	0.74
	NA	0.82	1.00	0.82
BC	WW	0.74	0.92	0.81
	NA	0.78	1.00	0.78
OT	WW	0.74	0.92	0.81
	NA	0.82	1.00	0.82
Average	WW	0.72	0.92	0.78
	NA	0.81	1.00	0.81

Table 3. It is confirmed that F_{RH} of WW ($= 0.78$ on average) is smaller than that of NA ($= 0.81$ on average), which indicates a more significant effect of storm avoidance in WW.

Moreover, around $P = 10^{-1} \sim 10^{-2}$ in Fig. 5a, which ships frequently encountered, a smaller value of F_{RH} (0.7) is clarified compared with that around $P = 10^{-5}$. It should be noted that the effect around $P = 10^{-1} \sim 10^{-2}$ is more important during the evaluation of fatigue strength.

5 Wave loads

5.1 Distribution of maximum value of *VBM* acted on individual ships

The vertical bending moment (*VBM*) that acted on ships in service is estimated by using the environmental parameters in the short-term sea, which consist of the significant wave height (*H*), the average wave period (*T*), the relative wave direction (χ), and the ship speed (*V*). The loading condition is assumed to be a full load for all ships.

The linear strip method [23, 32] is utilized to calculate the *VBM*, where the nonlinearity of the hull form and the hogging/sagging difference of the *VBM* is neglected.

The procedure for obtaining the standard deviation in the short-term sea and the long-term maximum expected value using actual data is shown below and in Fig. 7

1. Calculate the response amplitude operator (RAO) of the *VBM* utilizing the strip method.
2. Obtain the standard deviation of *VBM* in short-term sea *R* by linear superposition of the *RAO* and the wave spectrum. The *R* can be solved by the function of *H*, *T*, χ and *V*. Generally, it is applied to the IACS recommended wave spectrum [29].
3. Collect the time histories $H(t)$, $T(t)$, $\chi(t)$, and $V(t)$ of the wave conditions that ships encountered from the AIS data and wave data, where the time interval Δt is set to
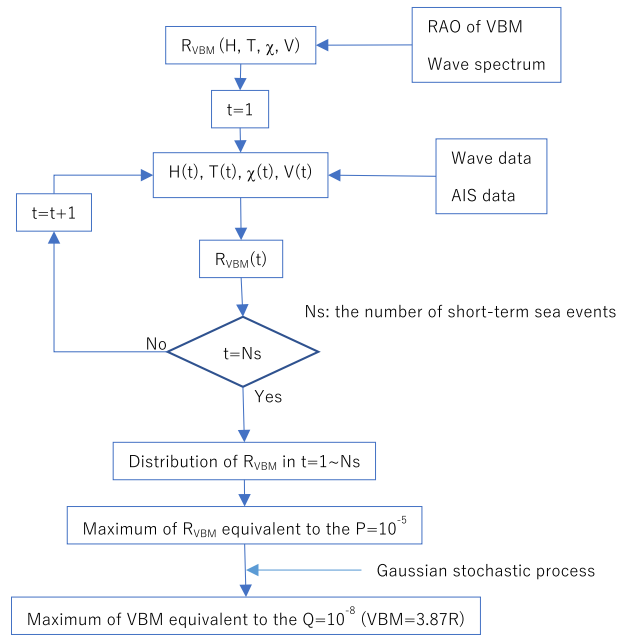

Fig. 7 Flow chart for long-term prediction of *VBM* using the actual data

1 h which matches the duration of the short-term sea condition.

4. Substitute $H(t)$, $T(t)$, $\chi(t)$, and $V(t)$ into the *R* to obtain the time history of $R(t)$.
5. Search the maximum value of the *R* in the target period which corresponds to the worst short-term sea condition. The exceedance probability *P* of the worst short-term sea condition is assumed to be $P = 10^{-5}$.
6. Solve the maximum expected value of 1/1000 in the worst short-term sea. Based on the assumption of the narrow-band response, the maximum expected value of 1/1000 can be derived according to Eq. 7, which follows the Gaussian stochastic process. The maximum expected value of 1/1000 for the worst short-term sea is equivalent to the long-term probability of exceedance $Q = 10^{-8}$.

$$VBM\left(Q = 10^{-8}\right) = 3.87R \tag{7}$$

The *VBMs* for 17,435 target ships are calculated by performing the above procedures (1–6) for each ship independently. As it is difficult to obtain the exact hull form data for all the 17,435 ships, an approximate hull information for each ship is generated by expanding or reducing the hull form data of the base model ship, considering the ratio of Length (*L*), Breadth (*B*), and draft (*d*) between the target ship and base model ship. The base model ship has a typical hull form of a post-Panamax for the container ship and a cape-size for the bulk carrier and oil tanker [12]. The information about

L, B, and d for all the 17,435 ships can be found in the AIS data.

Figure 8 shows the maximum expected value of the *VBM* acting on ships in service. DLA is the long-term predicted value corresponding to $Q = 10^{-8}$ by the guideline [31]. The *VBM* acting on ships in service is lower than the long-term prediction value. This can be explained by the effect of storm avoidance operations. Especially for container ships, it is clearly observed that the operational effect tends to increase with the increment of ship size.

Figure 9 shows the maximum *VBM* acted on ships in NA. Concerning the container ships and the oil tankers, *VBM* in NA is larger than that in WW on average. While for the bulk carriers, the *VBM* in NA is almost the same as that in WW.

Based on Figs. 8 and 9, a significant operational effect on *VBM* is clearly observed even though a large variation still exists among the individual ships. Moreover, since the period of data is 2 years at maximum, it is difficult to present the comparison between the actual data and DLA in a period of 25 years. Therefore, we considered normalizing the *VBM* data of individual ships and performing statistical analysis using the data of all ships as a sample. In the next section, long-term prediction using actual data is discussed.

5.2 Long-term prediction of *VBM*

Long-term predictions are performed using the actual data obtained by AIS and nowcast wave data. The physical quantity of *VBM* is different depending on ship size. To exclude the influence of different ship sizes, the normalized *VBM* (see Eq. 8) is utilized for the following long-term estimation. In this study, the long-term prediction value calculated by direct load analysis (VBM_{DLA}) is applied. VBM_{DLA} is shown in Figs. 8 and 9 marked by "Direct Load Analysis".

$$VBM = \frac{VBM_{ACTUAL}}{VBM_{DLA}} \tag{8}$$

VBM_{ACTUAL}: *VBM* estimated using AIS data and wave data for the actual ships. VBM_{DLA}: Long-term maximum expected value of *VBM* calculated by direct load analysis [31]

The number of short-term seas that ships encountered during the target period is shown in Table 4. The amount of data for performing the long-term prediction is sufficient.

The long-term distribution of *VBM* was obtained by accumulating the short-term distribution based on the Gaussian stochastic process. The short-term probability of exceedance q of *VBM* is calculated according to Eq. 9.

$$q(x > x_1) = exp\left(-\frac{x_1^2}{2R^2}\right) \tag{9}$$

R: standard deviation of *VBM* in the short-term sea.

The long-term exceedance probability (Q) is expressed by Eq. 10 using the probability density function of the R during long-term (p).

$$Q(x > x_1) = \int_0^\infty q(x > x_1)p(R)dR \tag{10}$$

Figure 10 shows the long-term exceedance probabilities of *VBM*. The maximum expected values at $Q = 10^{-8}$ are under 1.0 which is equal to VBM_{DLA}. It is found that the safety margin of the predicted value of DLA is 20% to 40%, which is more significant than that ($S.M. = 15\%$) of ocean wave data. It is confirmed that the *VBM* is mitigated due to the safe operation. Concerning CS and OT, the shape of the long-term distributions is almost the same between WW and NA. Concerning BC, the shape is different depending on the sea area. The ultimate *VBM* below $Q = 10^{-8}$ in exceedance probability in WW is larger than that in NA. The bulk carriers are likely to encounter severe sea conditions outside the North Atlantic.

Figure 11 shows the *VBM* with the exceedance probability $Q = 10^{-8}$, in which the influence of the kind of ship, sea area, and presence or absence of the operation is emphasized. It is proved that the operational effect due to sea area and storm avoidance exists for each kind of ship.

The F_{OP}, which is the operational coefficient on wave load, can be obtained by Eq. 3. F_R, which is the component of F_{OP} related to storm avoidance, can be obtained by Eq. 4. These operational coefficients on wave load are shown in Table 5. The effects of storm avoidance are shown in Fig. 12 where the effect is expressed as "1-F_R" or "1-F_{RH}". It is found that the effect of storm avoidance of WW is larger than that of NA on average. The influence of F_R depends on the ship type. The F_R of WW is smaller than that of NA for CS and OT. However, for BC, the larger F_R is achieved for WW. A detailed explanation on this phenomenon is presented in the next session.

It is found that the effect of storm avoidance on *VBM* is less than that of wave height. It also can be noticed that the F_{RO} exceeds 1.0 in Table 3. F_{RO} can be obtained by Eq. 5. It is clarified that the effect of storm avoidance on wave height is 15% or more, but the effect on *VBM* may be less than 15%, depending on the sea area and ship type. According to Fig. 12, it is known that, due to the influence of the ship operational factors such as the average wave period (T), the relative wave direction (χ), and the ship speed (V), the reduction of wave load caused by the storm avoidance is smaller than the reduction of significant wave height.
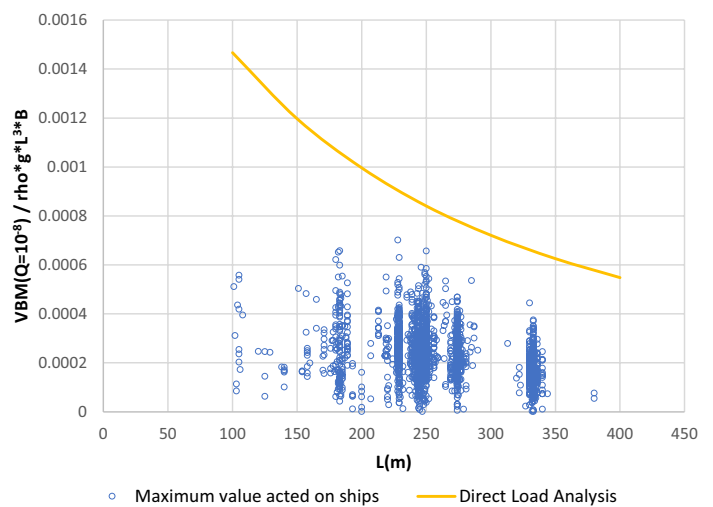
Fig. 8 The maximum expected value of *VBM* acting on actual ships in a worldwide sea area
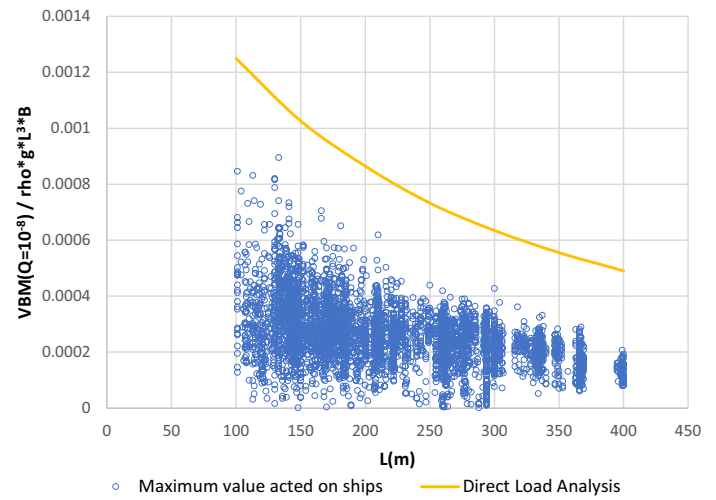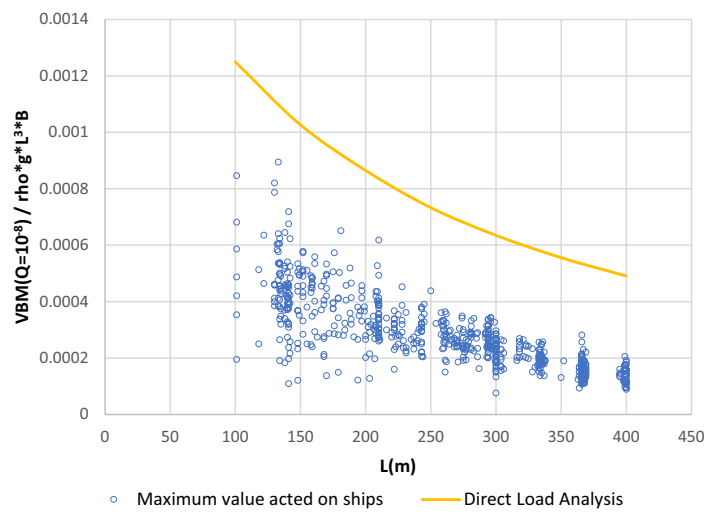

a Container Ship
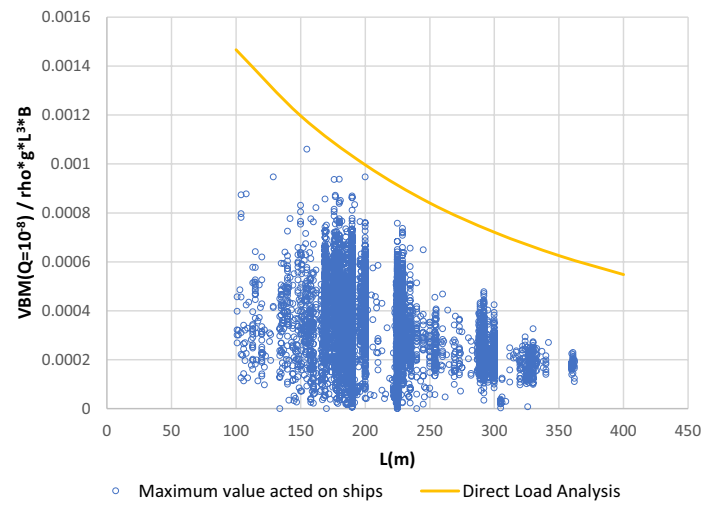
b Bulk Carrier
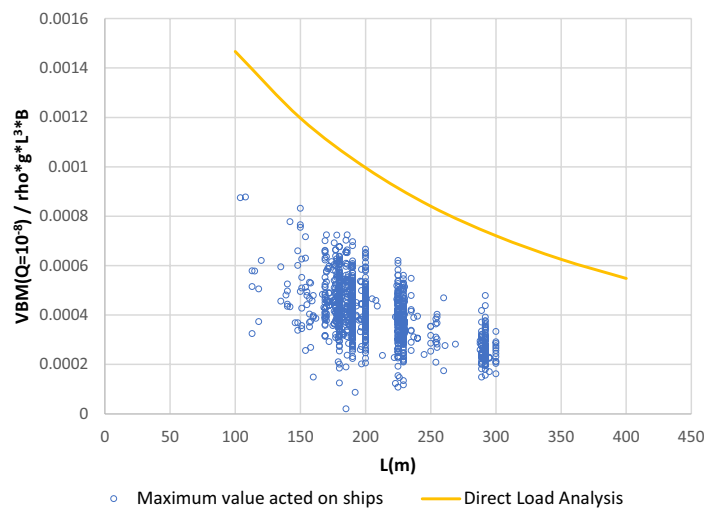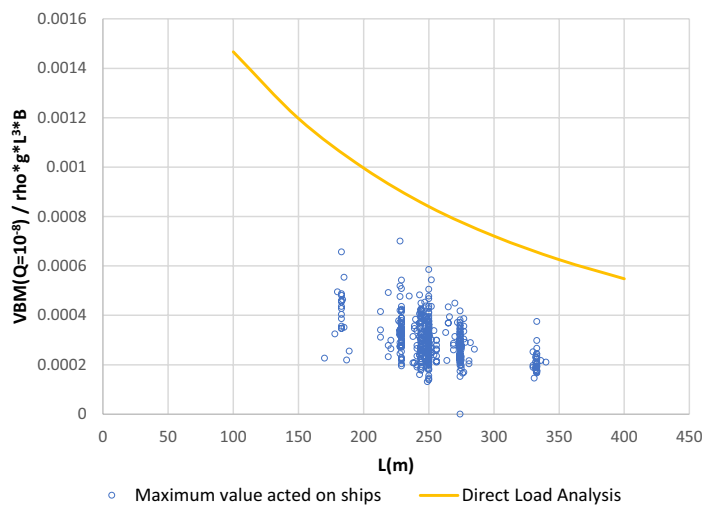

c Oil Tanker

Fig. 9 The maximum expected value of *VBM* acting on actual ships in North Atlantic

a Container Ship

b Bulk Carrier

c Oil Tanker

Table 4 The number of short-term sea that ships encountered

Ship type	CS	BC	OT
WW	21,398,577	58,701,760	13,193,588
NA	801,388	1,094,482	327,654

Fig. 11 The maximum expected value of *VBM* based on the actual data

Fig. 10 The exceedance probability of *VBM* based on the actual data of all ships carriers

5.3 Analysis of *VBM* on bulk carriers

5.3.1 Difference of probability distribution by ship size

In Fig. 10, it is observed that the shape of the long-term

distribution of the bulk carriers is different from that of other ship kinds. To clarify the reason of this difference, the long-term distributions divided by the ship size were calculated. Table 6 shows the number of short-term seas obtained by AIS and wave data for each category of ship size.

Figure 13 shows the long-term distributions. The shape of the long-term distribution for $L = 100$ m ~ 280 m is not so different from Fig. 10b, but for $L = 280$ m over, the distribution is similar to that of CS and OT which is shown in Fig. 10a and c. According to Fig. 13, regarding the small size BC, the severe wave load is acted over the worldwide sea area. It is known that the optimum wave load for ship design can be determined by properly classifying the ship's kind, sea area, and ship size.

5.3.2 The sea area where the ship experienced a severe wave load

Figure 14a–c shows the location where the maximum *VBM* of the individual ship is observed. Figure 14 shows the normalized *VBM* by Eq. 8. Regarding CS and OT, severe wave load is usually observed in the NA. However, regarding BC, severe wave load cases are widely distributed for example in the North Pacific and the Southern Hemisphere. This explains the reason for the difference in long-term distribution shape between Fig. 10a–c.

6 Conclusion

Utilizing the big data on the actual seam including AIS data and global ocean wave data, the vertical bending moment (*VBM*) in wave acting on the actual ships was clarified. The long-term prediction was performed based on the short-term analysis of *VBM* on actual ships in the worldwide sea area.

The effect of storm avoidance operations on wave height is about 22% in the worldwide sea area. It is greater than

Table 5 The operational coefficients on wave load (F_{OP}) and its component

		F_{OP}	F_A	$F_R (= F_{OP}/F_A)$	F_{RH}	$F_{RO} (= F_R/F_{RH})$
CS	WW	0.74	0.92	0.81	0.74	1.10
	NA	0.88	1.00	0.88	0.82	1.07
BC	WW	0.84	0.92	0.91	0.81	1.12
	NA	0.84	1.00	0.84	0.78	1.07
OT	WW	0.74	0.92	0.81	0.81	1.00
	NA	0.92	1.00	0.92	0.82	1.11
Average	WW	0.77	0.92	0.84	0.78	1.07
	NA	0.88	1.00	0.88	0.81	1.09
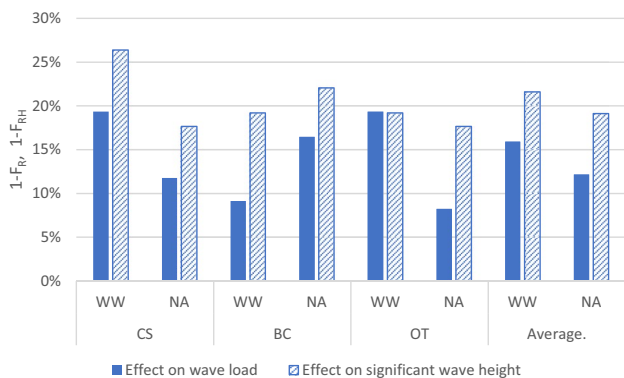
Fig. 12 The effects of storm avoidance on wave load (*VBM*) and wave height

Table 6 The number of short-term sea that the Bulk Carriers encountered

Size(*L*)	100~220 m	220~280 m	280~370 m
WW	29,259,619	17,928,302	11,513,839
NA	569,596	372,867	152,019

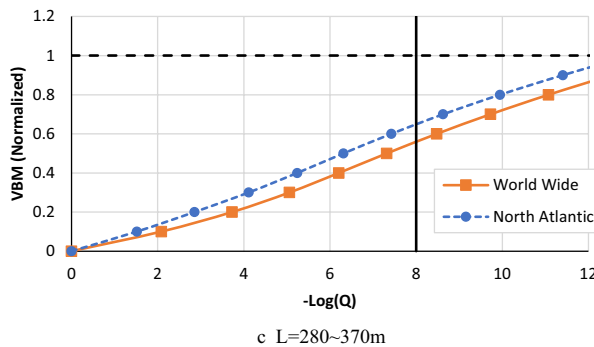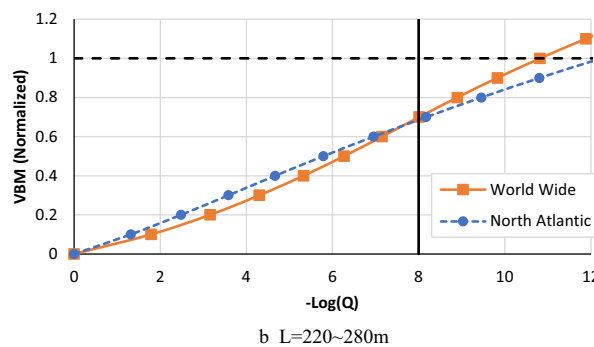**a** L=100~220m

b L=220~280m

c L=280~370m

Fig. 13 The exceedance probability of *VBM* based on the actual data of bulk carriers

that in North Atlantic (19%). The effect on *VBM* in the worldwide sea is about 16%. It is also greater than that in North Atlantic (12%). The effect of storm avoidance is more significant in WW compared with NA. The effect on *VBM* shows the dependency on the ship type. Container ships, oil tankers, and large-size bulk carriers usually encounter the severe wave load at the North Atlantic. But for small-size bulk carriers, the severe wave load can be observed in the worldwide sea area.

The effect of storm avoidance on *VBM* is less than that of wave height. The effect of storm avoidance on wave height is 15% or more, but the effect on *VBM* may be less than 15% depending on the sea area and ship type. Moreover, the influence of ship operational factors such as the average wave period (*T*), the relative wave direction (χ), and the ship speed (*V*) is validated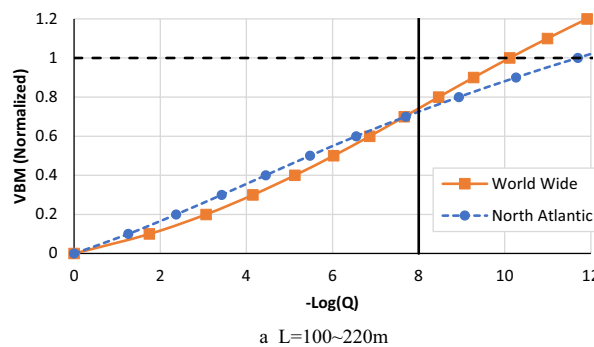 as well. Larger reduction of significant wave height due to the storm avoidance is observed compared with that of the wave load.

By applying the achievement of this study, it is possible to refine the safety factor of hull strength more accurately.
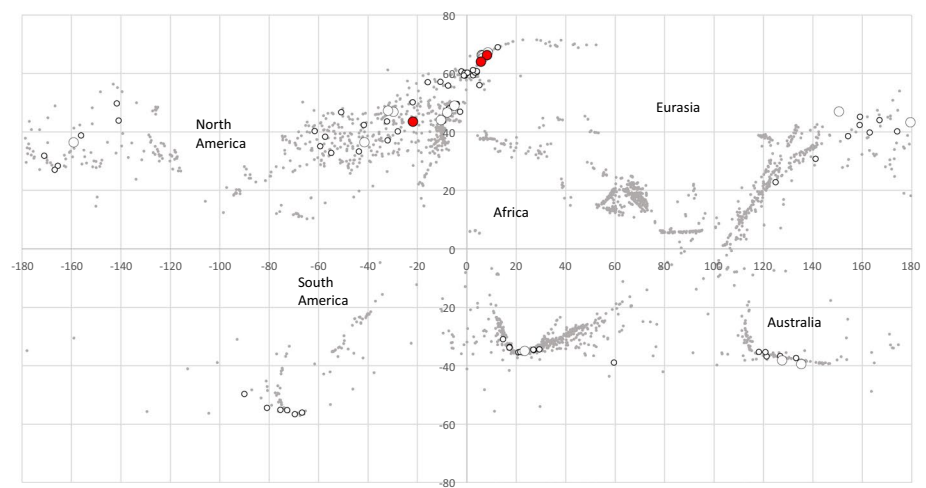
Fig. 14 Distribution of location where maximum *VBM* acted on each ship. (*VBM* = 0.5 ~ 0.6: Dot, *VBM* = 0.6 ~ 0.7: Open/Small, *VBM* = 0.7 ~ 0.8: Open/Big, *VBM* = 0.8 ~ : Solid/Big)
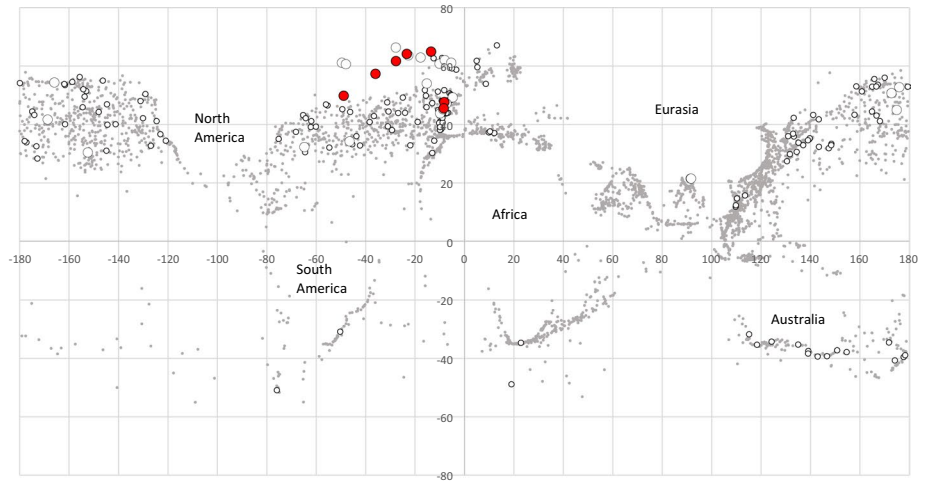
a Container Ship
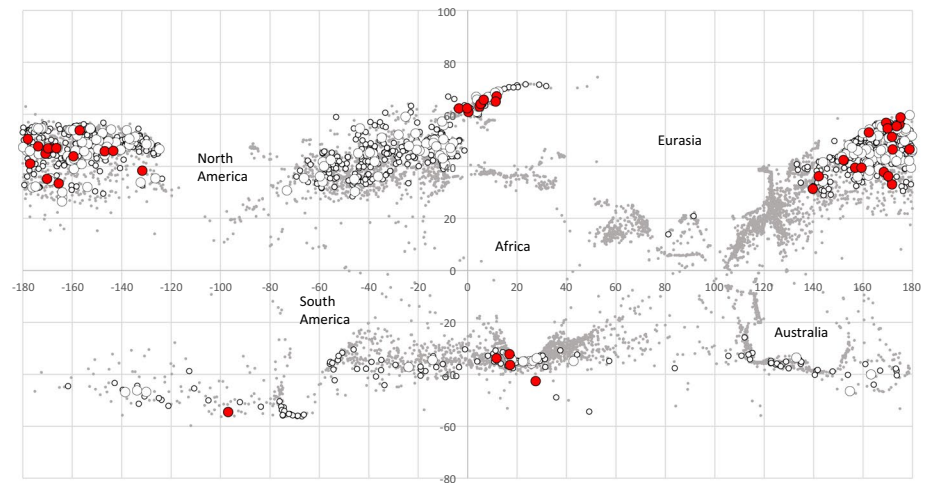
b Bulk Carrier

c Oil Tanker

Furthermore, as a future prospect, by using actual wave loads, it is expected to establish a more accurate fatigue life evaluation method than the full-spectrum analysis, and to design and construct lightweight ships environmentally friendly.

References

1. Soares CG (1990) Effect of heavy weather maneuvering on the wave induced vertical bending moments in ship structures. J Ship Res 34(1):60–68
2. Vettor R, Soares CG (2016) Assessment of the Storm Avoidance effect on the Wave Climate along the Main North Atlantic Routes. J Navig 69(1):127–144
3. International Association of Classification Societies (IACS) (2015) Unified Requirement S11A, Longitudinal Strength Standard for Container Ships
4. Eriksen T, Greidanus H, Delaney C (2018) Metrics and provider-based results for completeness and temporal resolution of satellite-based AIS services. Marine Policym 93:80–92
5. Vitali N, Prpic-Orsic J, Soares CG (2020) Coupling voyage and weather data to estimate speed loss of container ships in realistic conditions. Ocean Eng 210:106758
6. Tu E, Zhang G, Rachmawati L, Rajabally E, Huang GB (2018) Exploiting AIS data for intelligent maritime navigation: a comprehensive survey from data to methodology. IEEE Trans Intell Transport Syst 19(5):1559–1582
7. Miratsu R, Fukui T, Matsumoto T, Zhu T (2019) Quantitative evaluation of ship operational effect in actually encountered sea states, Proceedings of the 38th International Conference on Offshore Mechanics and Arctic Engineering, OMAE2019-95121
8. Sasmal K, Miratsu R, Kodaira T, Fukui T, Zhu T, Waseda T (2021) Statistical model representing storm avoidance by merchant ships in the North Atlantic Ocean. Ocean Eng 235:109163
9. Ruth E, Thompson I (2022) Comparing design assumptions with hindcast wave conditions and measured ship speed and heading. Ocean Eng 247:110613
10. IMO (2007) SN/Circ.227 and resolution MSC.74(69), annex 3
11. Oka M, Takami T, Ma C (2018) Estimation of wave loads acted on ships in service based on AIS Data. Evaluation of operational effects on the maximum loads. J Jpn Soc Naval Arch Ocean Eng 28:89–97
12. Oka M, Takami T, Ma C (2019) Evaluation method for the maximum wave load based on AIS and hindcast wave data, Proceedings of the 14th International Symposium on Practical Design of Ships and other Floating Structures, pp 308–320
13. Korvin Kroukovsky BV (1955) Investigation of ship motions in regular waves, SNAME
14. Newman J (1964) A slender-body theory for ship oscillations in waves. J Fluid Mech 18(4):602–618
15. Tasai F, Takagi M (1969) Response theory and calculation method in regular waves, 1st Symposium on Seakeeping, The Society of Naval Architects of Japan, pp 1–52
16. Faltinsen O (1971) A rational strip theory of ship motions, Part II. Technical Report, University of Michigan
17. Salvesen N, Tuck EO, Faltinsen O (1970) Ship motions and sea loads, Annual Meeting of the Society of Naval Architecture and Marine Engineers (SNAME), New York
18. Kashiwagi M, Ikeda T, Sasakawa T (2010) Effects of forward speed of a ship on added resistance in waves. Int J Offshore Polar Eng 20(3):196–203
19. Kashiwagi M (2017) Enhanced unified theory with forward-speed effect in the inner free-surface condition, Proceedings of the 32nd International Workshop on Water Waves and Floating Bodies (IWWWFB), Dalian, China
20. Kashiwagi M (2022) Enhanced unified theory with forward-speed effect taken into account in the inner free-surface condition. J Ship Res 66(1):1–14
21. Amini-Afsha M, Bingham HB (2021) Added resistance using Salvesen-Tuck-Faltinsen strip theory and the Kochin function. Appl Ocean Res 106:102481
22. Xia J, Wang Z, Jensen JJ (1998) Non-linear wave loads and ship responses by a time-domain strip theory. Mar Struct 11:102–123
23. Ohmatsu S, Matsui S (2019) On the improvement of approximate calculation method of diffraction potential in strip method, The report of National Maritime Research Institute 19(1): 79–89
24. Matsui S, Murakami C, Oka M (2017) Validation of the Nonlinear Wave Load Analysis Program NMRIW-II in Comparison with Experiments—Ship Responses in Regular Wave—, The report of National Maritime Research Institute 17(3): 81–164
25. Matsui S, Murakami C, Hayashibara H, Fueki R (2019) Development of Direct Load and Structure Analysis and Evaluation System on Whole Ship DLSA-Basic for Ship Structural Design, The report of National Maritime Research Institute 19(3): 1–21
26. The Japan Meteorological Agency (JMA): Global Spectral Model/Grid Point Value, http://www.jmbsc.or.jp/jp/online/file/f-online20100.html
27. Bishop RED, Price WG (1979) Hydroelasticity of Ships, pp 343, Cambridge University Press
28. Hogben N, British Maritime Technology Ltd, Dacunha NMC, Olliver GF (1986) Global Wave Statistics, Unwin Brothers Limited, London
29. International Association of Classification Societies (IACS) (2001) Recommendation No. 34, Standard Wave Data
30. exactEarth Ltd: https://spire.com/exactearth-data-licence/ (Accessed on 2022.3)
31. Class NK (2022) Guidelines for Direct Load Analysis and Strength Assessment (Edition 2.0)
32. NMRIW-Lite Web: https://cloud-trial.nmri.go.jp/portal/pub/lite-web